Int. J. Electrochem. Sci., 9 **(2014)** 6305 - 6327

International Journal of
ELECTROCHEMICAL
SCIENCE
www.electrochemsci.org

Nonlinear Structural Model of the Battery

Nikolay Galushkin[*], *Nataliya Yazvinskaya, Dmitriy Galushkin*

Don State Technical University, Laboratory of electrochemical and hydrogen energy, 147 Shevchenko Street, Town of Shakhty, Rostov Region, Russia, 346500.
[*]E-mail: galushkinne@mail.ru

Received: 26 July 2014 / *Accepted:* 18 August 2014 / *Published:* 25 August 2014

A nonlinear structural model of the battery that can be used for modeling the operation of alkaline, acid, and lithium-ionic batteries is constructed. This model retains all the advantages of traditional structural models: namely, it contains as many parameters as can be determined from experimental studies for the battery as a whole. This model, as well as all structural models, is graphic and understandable from both electrochemical and electrotechnical points of view. However, the proposed nonlinear structural model can be used for modeling the operation of the battery at high currents that are usually found in various modes of their operation. This is the main difference between the given model and traditional structural models which are used only in the theory of an impedance, that is, during the use of small alternating currents.

Keywords: battery, modeling, structural model, lithium-ion, nickel–cadmium

1. INTRODUCTION

Currently, in spite of many different models of a battery, only a few methods deal with the development of such models, namely the statistical method, dynamic method, constructive method, and structural method.

The statistical method dealing with the development of a battery model is used during the first stage of the study, when there is little information available on the battery under study. Within the framework of the given method, the battery model is regression function on the basis of the experimental data available. Usually, a polynomial or a more complicated functional dependence, selected on the basis of certain theoretical considerations [1-3], is considered a regression function. One of the drawbacks of such a method is that the obtained models are applicable only for such modes of battery operation, that is, for those from which they are obtained. However, the given models are the criteria that are used for the development of more complicated and more global models.

Within the framework of the dynamic method, the battery model is developed on the basis of the known laws of the transport of components (ions, electrons, and neutral particles) in different media [4-10]. In this case, the battery model is divided into sub-models. Each of these sub-models describes the processes in different mediums: in a liquid phase of inter-electrode space, in a liquid phase inside a porous electrode, in the metal matrix of a porous electrode, and at phase boundaries. The given method is the most fundamental one. The battery models obtained with the help of the dynamic method are considered the most global ones. The most difficult part of the given models is a sub-model that describes the processes in a porous electrode. The given processes are described within three generally accepted models: macrohomogeneous [4-9], single pore [10] or electrotechnical [11]. The most advanced of the given models is the macrohomogeneous model. The system of equations for the macrohomogeneous model differs to a great extent for the weak [4-6] and concentrated electrolytes [7-9]. Researchers using dynamic battery models in electrotechnical systems usually indicate two disadvantages of these models [12]. First, the models contain very many parameters that describe a large number of local processes and phenomena. As a rule, such parameters for a particular battery are either impossible or very difficult to be measured in practice. For example, parameters of function Butler–Volmer and other local parameters inside of a porous electrode (which are used in models) cannot be directly measured. These local parameters are determined from experimental studies on the electrode surface. However, it is not entirely obvious that the local parameters found are equivalent to the corresponding parameters inside of a porous electrode. Second, these models are very intricate and complicated for practical use. Therefore, to simulate the operation of batteries in the structure of a hybrid electric vehicle (HEV), statistical models are used more often [13,14].

When the ion transport details are not very significant for the solved problem, the battery model is developed on the basis of both theoretical and experimental assumptions. Such models are a great many [15-17], and they differ based on the assumptions or simplifications made, excluding the necessity of a consequential provision for component transport. The given constructive method enables the simplification of complicated dynamic models to a great extent. A drawback of the given method is that the model obtained is true only within the framework of the formulated problem. These models have no global character, as evident in the case of the dynamic models.

It is quite natural that there is no clear border between the constructive models and dynamic models under consideration, as well as between the constructive models and statistical models. This border is subjective in many aspects.

In structural modeling, the object or process under investigation is treated as a system that consists of sub-systems or elements. The studied process is divided into elements as a result of a study of the process and its division into different stages; each stage of the process is assigned with one or several structural elements. The elements of the structural model can be categorized as standard electrotechnical elements (resistances, capacitances, etc.) and specific electrochemical ones (Warburg impedance, etc.). In a structural model, the elements are connected according to an understanding of the mechanism of a studied process [18-20]. Structural models possess some advantages [20].

First, structural models have as many parameters as can be determined from experimental studies for the battery as a whole. Thus, there is no need to separately carry out experimental studies of the local phenomena on the surface and inside of a porous electrode.

Second, structural models are always very graphic and understandable from an electrotechnical as well as an electrochemical standpoint, which is their undeniable advantage.

A drawback of this method is that structural modeling is used only in impedance theory, that is, in models with small alternating currents.

In this article we construct a nonlinear structural model of the battery. The model can be used to simulate the operation of the battery at high currents that are usually found in various modes of their operation. The model can be used for batteries of any electrochemical system. Nevertheless, in this article, the battery model is based on empirical data for alkaline batteries. However, all theoretical conclusions will, in many instances, also be true for the batteries of any electrochemical system.

2. ANALYSIS OF EMPIRICAL RELATIONS DESCRIBING THE ACCUMULATORS' DISCHARGE AT DIRECT CURRENT

We will commence developing a structural model of an alkaline accumulator based on an analysis of an empirical relations describing the discharge of alkaline accumulators at direct current. These relations are numerous and the most examined. In general, this is the primary reason for selecting them for the beginning of the alkaline accumulator structural model development.

It is highly possible that among the most examined empirical relations describing voltage change at the accumulator terminals during their discharge by direct current shall be following relations:

- Shepherd [21]

$$U = E - RI - K\left(\frac{q}{C-q}\right)I + A\left[exp\left(-B\frac{q}{C}\right)-1\right], \quad (1)$$

- Tremblay [13]

$$U = E - RI - K\left(\frac{q}{C-q}\right) + A\left[exp\left(-B\frac{q}{C}\right)-1\right], \quad (2)$$

- generalized empirical relation (GER) [3,14, 22],

$$U = E - RI - \left(\frac{Dq + KqI}{C-q}\right) + A\left[exp\left(-B\frac{q}{C}\right)-1\right], \quad (3)$$

where E–accumulator EMF (electromotive force); R–internal activation-ohmic accumulator resistance; C–full accumulator capacitance; I–discharge current; K, A, and B–experimental constants and q–quantity of electricity, released by the accumulator, for the moment of voltage U measurement.

The Shepherd's equation (1) follows from the equation (3) at $D = 0$, and Tremblay's equation (2) at $K = 0$.

In addition to the earlier dependencies, there are many relations [1,23–25]. However, these relations, as a rule, are simplifications of the relations (1–3) or their possible approximations.

Equations (1–3) are obtained by the study of different types of accumulators. For example, initially obtained Shepherd's equation (1) was applied to acid accumulators, but currently, it is also used for the NiCd, Li-Ion, and NiMH accumulators' category [14,26]. In spite of the fact that the given

relations are the most examined, they differ to a great extent; hence, the aim of this article is to analyze these differences and find the internal correlation between them.

In the article [27], it is experimentally proved that generally the equation describing the discharge characteristics of electrochemical cells has the following view

$$U = E - RI - Kf_1(I,q) + Af_2(q). \quad (4)$$

Empirical dependencies (1–3) correspond to this requirement. Hence, in general, these dependencies by themselves represent the sum of four summands (4). Consequently, on the basis of these dependencies, the accumulator can be considered four-series connected elements, as evident in Fig.1.

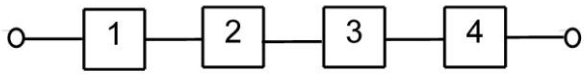

Figure 1. Block diagram of accumulator structural model: (1) accumulator EMF; (2) activation-ohmic element; (3) element, determining discharge polarization and (4) relaxation element

The first element represents the ideal source of continuous EMF. The second element describes the activation-ohmic part in accumulator operation. The third element is transformed into zero at $q = 0$ and grows along the absolute value, as the accumulator discharges; that is, this element describes the change of voltage related to the degree of accumulator discharge. Therefore, we have conditionally named this voltage change *accumulator discharge polarization*. The final element describes transitional processes developing in the accumulator at its closure to discharge. Hence, we have conditionally named the change of voltage corresponding to this element *relaxation polarization*. Analytical relations describing the fourth element operation have a similar view in all equations (1–3).

Let us analyze analytical relations for each of these elements. The first element represents by itself the ideal source of continuous EMF. It is described by a constant. There is no doubt in the accuracy of this description and necessity of the first element. The second element describes the ohmic resistance of electrolyte in the interelectrode space and in electrodes, as well as resistance related to activation processes. Let us start with a detailed analysis of the most complicated third element.

3. DISCHARGE POLARIZATION

Summands describing discharge polarization differ mostly in various empirical relations. Thus, in Tremblay equation (2), the discharge polarization is described by the summand

$$U_P = -K\frac{q}{C-q}, \quad (5)$$

in Shepherd's equation (1), by the summand

$$U_P = -K\frac{qI}{C-q}, \quad (6)$$

in GER (3), by the summand

$$U_P = -\frac{Dq + KqI}{C - q}. \qquad (7)$$

In [23], an interesting method to check the adequacy of analytical relations to experimental data was used. Following this method, the constant coefficients were determined in the relations under study in such a way as to ensure the most exact correspondence of these relations to experimental points, i.e. the optimal coefficients and the corresponding optimal curves were determined. Three situations are possible in this method.

First, if for a series of discharge modes (at different currents), the dispersion of experimental points in all the series of located optimal curves are big then this analytical dependence does not correspond to the nature of studied object.

Second, if the dispersion for all the series of modes are small, but optimal coefficients have different meanings for different discharge modes, then these coefficients are not constants at all but functions of discharge modes shall be changed to functional dependencies, i.e. in this case, the analytical relations or particular summands need advancement.

Third, if optimal coefficients in the total in relation or in a particular summand do not change depending on the mode of discharge, then these relations do not require advancement and correctly describes the studied object.

We experimentally checked these conclusions for KCSH 8 and KSX 25 accumulators.

The following discharge modes were studied for KSX 25 accumulator:

- Mode 1 – discharge with the current 25 A for 8 $A \cdot h$, then 5 A current to 0.5 V;
- Mode 2 – discharge with the current 25 A for 13 $A \cdot h$, then 5 A current to 0.5 V;
- Mode 3 – discharge with the current 25 A for 4 $A \cdot h$, then 13 A current for 10 $A \cdot h$, then 5 A current to 0.5 V;
- Mode 4 – discharge with the current 5 A to 0.5 V;
- Mode 5 – discharge with the current 25 A to 0.5 V;
- Mode 6 – discharge with the current 5 A for 15 $A \cdot hr$, then 25 A current to 0.5 V.

Optimal parameters for Tremblay (2) and Shepherd's (1) relations, corresponding to the indicated experimental discharge modes, were detected using Levenberg-Marquardt optimization method and presented in Tables 1-2.

Table 1. KSX 25 accumulator discharge curves' optimal parameters for Tremblay relation (2)

Parameters	Discharge modes					
	No. 1	No. 2	No. 3	No. 4	No. 5	No. 6
E (V)	1.391	1.384	1.392	1.393	1.386	1.387
R (mOhm)	3.66	4.44	3.35	6.88	3.88	6.68
K (mV)	5.233	5.475	6.027	5.314	5.124	5.571
A	0.121	0.124	0.121	0.122	0.123	0.124
B	3.81	3.75	3.58	3.54	3.69	3.55
C (Ah)	31.08	30.63	30.33	31.07	30.32	29.50
$D_I 10^4$ [a]	0.52	0.90	0.76	0.88	0.81	0.83

[a] D_I - experimental points dispersion

Table 2. KSX 25 accumulator discharge curves' optimal parameters for Shepherd's relation (1)

Parameters	Discharge modes					
	No. 1	No. 2	No. 3	No. 4	No. 5	No. 6
E (V)	1.392	1.386	1.391	1.391	1.385	1.392
R (mOhm)	3.46	4.11	3.42	6.50	3.62	6.73
K (mOhm)	2.520	2.934	3.347	2.554	0.550	0.519
A	0.122	0.123	0.129	0.126	0.124	0.130
B	3.580	3.635	3.917	3.691	3.447	3.783
C (Ah)	31.12	30.31	30.43	30.31	30.24	29.80
$D_I\ 10^4$ [a]	1.51	1.04	1.15	1.28	0.91	1.81

[a] D_I - experimental points dispersion

As shown in Table 1, for Tremblay equation, the summand *K* do not change greatly during transition from one mode to another (relative error 6%). Meanwhile, in Shepherd's equation (Table 2), the alteration of summand *K* is significant, with an average of about 65%. This implies that for these accumulators, the relation (5) is true for discharge polarization in the broad range of discharge currents.

Relation (5) can be represented as discharge of a certain pseudo-condenser

$$U_P = -\frac{q}{C_{CR}}, \qquad (8)$$

where

$$C_{CR} = C_{CR0}\left(1 - \frac{q}{C}\right), \quad C_{CR0} = \frac{C}{K}. \qquad (9)$$

C_{CR} denotes pseudo-condenser capacitance, which decreases as the accumulator discharges.

In spite of the fact that electro-chemical and physical processes at accumulator and condenser discharge are principally different, these systems are similar from the electro-technical point of view.

During discharge of nickel-cadmium accumulator at the positive electrode, the following reaction occurs

$$NiOOH + H_2O + e^- \rightarrow Ni(OH)_2 + OH^-, \qquad (10)$$

and at the negative electrode, the following reaction occurs

$$Cd + 2OH^- \rightarrow Cd(OH)_2 + 2e^-. \qquad (11)$$

Reaction (10) causes decrease in oxidation degree of the nickel hydroxides, and consequently, it causes decrease in the equilibrium potential of the positive electrode. Reaction (11) causes increase in the oxidation degree of the cadmium hydroxides, and consequently, it causes increase in the equilibrium potential of cadmium electrode.

During discharge of the condenser, the positive charge decreases at the positive plate (due to electrons inflow), which causes decrease in the potential of the positive plate. At the negative plate of the condenser, the negative charge decreases (due to electrons outflow), which causes increase in the negative plate potential.

Consequently, if we are interested only in the dependencies between electro-technical

characteristics of the accumulator (current, voltage at the terminals, quantity of transferred electricity and time), then the results of accumulator and condenser discharge are equal, particularly in the decrease of the difference of potentials between the terminals. Then, it is natural that these different objects are described by equal analytic relations, describing similar electro-technical processes.

In complete series of articles [21,23,25], the discharge polarization is interpreted as voltage drop at the resistance according to Shepahrd's equation (1)

$$K\frac{q}{C-q}I = R_0 I \,. \qquad (12)$$

From the point of direct current discharge, such an interpretation appears quite acceptable; however, it leads to apparent contradictions if extended to other processes. For example, if the current in the process of discharge is cut, then the voltage drop at the resistance R_0 shall immediately disappear and voltage at the accumulator terminals would become equal to the charged accumulator EMF, independent of the amount of transferred electricity at discharge, which is the obvious contradiction to experiment. If we interpret discharge polarization as discharge of pseudo-condenser, then the discharge current cut-off shall cause voltage at accumulator terminals equal to charged accumulator EMF, minus voltage change at pseudo-condenser, which exactly corresponds to experience (relaxation processes, which are described by the fourth summand of the relations (4), are not considered).

The expression in the denominator of discharge polarization (5) describes the resource of the main current-forming reaction for a nickel-cadmium accumulator

$$\frac{1}{2}\mathrm{Cd} + \mathrm{NiOOH} + \mathrm{H_2O} \rightarrow \frac{1}{2}\mathrm{Cd(OH)_2} + \mathrm{Ni(OH)_2}\,. \qquad (13)$$

When $q \rightarrow C$, the discharge polarization grows rapidly in absolute value and accumulator terminals voltage drops rapidly, then it says about the exhaust of reaction resources (13) or just the same exhaust of reactions' resources (10,11). Reaction (10) keeps potential of a positive electrode at relatively continuous value (during the accumulator discharge), its exhaust shall cause the potential of the given electrode to other lower values. Similarly, the exhaust of reaction resource (11) at the negative electrode may cause the rapid increase of the electrode potential. All this is described by the expression in the denominator (5).

Thus, by the interpretation of discharge polarization (5) as the pseudo-condenser's discharge (8), another very important conclusion is made, namely: from the mathematical point of view, the current-forming reaction resource for nickel-cadmium accumulators can be correctly described by decrease of pseudo-condenser's (9) capacitance C_{CR} as the accumulator discharges. This fact was not intuitively apparent (opposite to the possibility of accumulator discharge description as discharge of a pseudo-condenser). This is a very important conclusion for modelling of the accumulator operation. In the modern accumulator models, the reaction resource is either not considered or is considered by introduction of the bounding inequality for q [4-8] alternative, which is a rough approximation to reality. As in this case, the transition from the state where reaction (13) is valid to the state where it is already exhausted should be instantaneous. In nature, all transitions of this type pass through the smoothly varying curves, even if we talk about small local amounts of active substance. The type of transition curve can be determined by a particular electro-chemical system. In this case, according to empiric dependency (8), the change of reaction (13) resource is described by the function (9).

4. ACCOUNTING OF THE IN-DEPTH CURRENT DISTRIBUTION IN POROUS ELECTRODE

If discharge polarization is described by Tremblay relations (5), then linear portions of discharge curves at the different discharge currents shall be approximately parallel because at this $q = q_{0,}$ the points at different discharge curves differ only by voltage drop at the activation-ohmic resistance, i.e. at RI. For KCSH 8 and KSX 25 accumulators, the discharge curves have this view at discharge currents up to $I = C_N$, Fig. 2. The discharge curves of such a type are characteristic for starter type accumulators. At these accumulators the shape of the discharge curves changes insignificantly at the change of discharge current in the broad range. If we examine the discharge curves of the accumulators with thick electrodes, Fig. 3, then it can be observed that discharge curves linear sections' inclination grows with the increase of discharge current value. Hence, these curves cannot be described by relations (5).

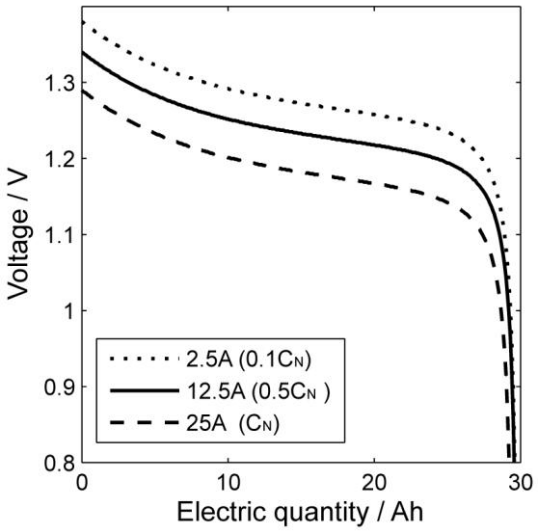

Figure 2. Experimental discharge curves of KSX 25 accumulator

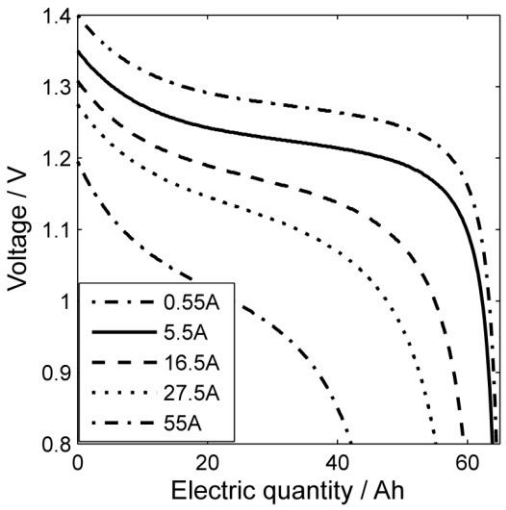

Figure 3. Experimental discharge curves of KPL 55 accumulator

Shepherd's equation assumes that the slope coefficient of the discharge curves' linear sections grows linearly (along the absolute value) with the growth of discharge current, as

$$-K\frac{I}{C-q}q=-kq\cdot \qquad (14)$$

Thus, Shepherd's equation, possibly, describes the discharge curves of accumulators with thick electrodes.

We discovered the optimal coefficients of Tremblay and Shepherd's equations for KPL 55 accumulator with thick pocket electrodes. The research was conducted for the following experimental modes of discharge:

- Mode 1 – discharge with the current 0.55 A ($0.01C_N$) to the voltage 0.8 V;
- Mode 2 – discharge with the current 5.5 A ($0.1\ C_N$) to the voltage 0.8 V;
- Mode 3 – discharge with the current 16.5 A ($0.3C_N$) to the voltage 0.8 V;
- Mode 4 – discharge with the current 27.5 A ($0.5\ C_N$) to the voltage 0.8 V;
- Mode 5 – discharge with the current 55 A (C_N) to the voltage 0.8 V.

The corresponding experimental discharge curves are shown in Fig. 3. The optimal parameters of relations (1, 2, 3) for KPL 55 accumulator are represented in Tables 3-5.

Table 3. KPL 55 accumulator discharge curves' optimal parameters for Tremblay relation (2)

Parameters	Discharge modes				
	No. 1	No. 2	No. 3	No. 4	No. 5
E (V)	1.44	1.44	1.44	1.44	1.44
R (mOhm)	73.0	16.0	8.0	6.0	4.6
K (mV)	12	13	32	50	62
A	0.120	0.118	0.120	0.120	0.153
B	6.50	6.50	6.50	6.70	6.27
C (Ah)	66.03	65.74	64.30	62.87	52.84
$D_I\ 10^4$ [a]	1.2	1.1	0.6	0.6	0.3

[a] D_I - experimental points dispersion

Table 4. KPL 55 accumulator discharge curves' optimal parameters for Shepherd's relation (1)

Parameters	Discharge modes				
	No. 1	No. 2	No. 3	No. 4	No. 5
E (V)	1.44	1.44	1.44	1.44	1.44
R (mOhm)	73.0	16.0	8.0	6.0	4.5
K (mOhm)	22.00	2.03	1.94	1.82	1.13
A	0.120	0.118	0.120	0.120	0.154
B	6.50	6.49	6.49	6.69	6.29
C (Ah)	66.03	65.73	64.30	62.86	52.84
$D_I\ 10^4$ [a]	1.60	0.64	0.75	0.54	0.46

[a] D_I - experimental points dispersion

Table 5. KPL 55 accumulator discharge curves' optimal parameters for Generalised empirical relation (3)

Parameters	Discharge modes				
	No. 1	No. 2	No. 3	No. 4	No. 5
E (V)	1.44	1.44	1.44	1.44	1.44
R (mOhm)	73.0	16.0	8.0	6.0	4.4
K (mOhm)	0.202	1.682	1.711	1.682	1.063
A	0.120	0.118	0.120	0.120	0.153
B	6.50	6.50	6.49	6.70	6.34
C (Ah)	66.03	65.74	64.30	62.87	52.85
D(mV)	12.00	3.75	3.76	3.75	3.69
$D_I\ 10^4$ [a]	1.2	0.6	0.5	0.6	0.4

[a] D_I - experimental points dispersion

From the Table 3, it can be observed that the coefficients *K* in Tremblay polarization discharge (5) strongly depend upon discharge current. Consequently, the Tremblay equation cannot describe correctly (at constant coefficients) the series of the KPL 55 accumulator discharge curves.

The coefficients *K* in the Shepherd's discharge polarization (Table 4) and the GER (Table 5) depend upon the discharge current: at low currents $I_p < 0{,}1C_N$ and at high currents $I_p > 0{,}5C_N$. Within the range of discharge currents from $I_p = 0{,}1C_N$ to $I_p = 0{,}5C_N$, the coefficients *K* have the approximately equal value (relative error 6% and 1%, respectively). Consequently, the Shepherd's equation (1) and the GER (3) correctly describe the KPL 55 accumulator discharge curves within the indicated range of discharge currents.

The accumulators for which discharge curves are described by Tremblay relations differ in thickness of electrodes from the accumulators for which discharge curves are described by the Shepherd's and GER equations.

For the thick electrodes during the increase of the discharge current, the depth of electro-chemical process penetration inside the porous electrode decreases [28,29], and consequently, the accumulator capacitance decreases because of the decrease in the active mass, which can be used in the electro-chemical process of discharge. But the decrease of accumulator capacitance shall cause the increase (by absolute value) of the discharge curve linear section slope coefficient. From a relation (8) follows

$$U_p = -\frac{q}{C_{CR}} = -kq. \qquad (15)$$

From equation (15), it can be observed that decrease of C_{CR} capacitance shall cause the increase of *k.* Because of this reason, we shall analyse in detail the influence of current distribution along the porous electrode depth on the type of discharge polarization.

5. CURRENT DISTRIBUTION MODELLING ALONG THE POROUS ELECTRODE DEPTH

Let us examine the case of continuous distribution of pseudo-capacitance along the depth of a porous electrode according to the active mass distribution. In this model, we shall not consider the ohmic and relaxation processes, corresponding to the second and fourth summands in formula (4). In addition, as we are only interested in linear section of discharge curve, we shall consider the pseudo-capacitance C_{CR} (modelling the work of main electro-chemical reaction in the accumulator (13)) as a constant. Nonlinearity of C_{CR} has great importance only in the end of accumulator discharge, but this section of discharge curve is not studied here.

Let us consider the surface of electrode as the point of beginning. An axis OX is directed perpendicularly inside the electrode. In this case, to determine the distribution of polarization along the depth of porous electrode, the macro-homogeneous model of porous electrode in the activation-ohmic mode is used [4-6]

$$\frac{\partial^2 U}{\partial x^2} = \rho \cdot s \cdot j(U), \qquad (16)$$

where ρ – specific resistivity to ion transport in depth of porous electrode; $\boldsymbol{s}$ – electrode porosity and $j(U)$ – discharge current density for porous matrix, corresponding to the main electro-chemical reaction (13).

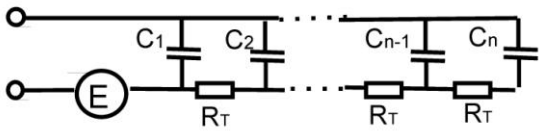

Figure 4. N-layer structural model of nickel-cadmium accumulator, not considering relaxation and ohmic elements of formula (4). R_T – resistance to ions' transport into the depth of an electrode along the liquid phase and active substance; C_i – distributed pseudo-capacitance in depth of porous electrodes corresponding to electro-chemical reaction (13) and E – accumulator EMF

In our case, according to the reaction modelling (13) as the pseudo-condenser discharge, the following expression for the current density can be obtained.

$$j(U) = C_{CRS} \cdot \frac{\partial U}{\partial t}, \qquad (17)$$

where C_{CRS} - superficial pseudo-capacitance inside the pores, corresponding to reaction (13).

Let's introduce the new constants, characterizing the accumulator as a whole

$$R_L = \frac{r}{L} = \frac{\rho}{S}, \qquad C_L = \frac{C_{CR}}{L} = \frac{C_{CRS} \cdot S_p}{L}, \qquad s = \frac{S_p}{S \cdot L}, \qquad (18)$$

where r – overall resistance of all the accumulator's electrodes to transport of ions into the depth of electrodes, both in liquid phase and in active substance; R_L – linear resistivity to transport of ions into the depth of porous electrode; C_{CR} – overall pseudo-capacitance of the accumulator corresponding to reaction (13); C_L – specific linear pseudo-capacitance; S – surface of electrodes; S_p –

inside surface of electrodes' pores and $2L$ – effective thickness of electrodes, i.e. average between thicknesses of positive and negative electrodes.

Considering (17,18) out of (16), we shall obtain

$$\frac{\partial^2 U}{\partial x^2} = R_L C_L \frac{\partial U}{\partial t}. \qquad (19)$$

This equation is the continuous analogue of discrete model of an accumulator with porous electrodes, Fig. 4 [30].

Let's solve the equation (19) using the standard boundary conditions, where I – discharge current

$$I = \frac{1}{R_L}\frac{\partial U}{\partial x}\bigg|_{x=0}, \qquad \frac{\partial U}{\partial x}\bigg|_{x=L} = 0, \qquad U(x,0)\big|_{t=0} = E. \qquad (20)$$

Considering $q = It$, we obtain

$$U = E - \frac{IR_L}{2L}(x-L)^2 - \frac{q}{C_L L} + \frac{IR_L}{2L}L^2 - \\ - 2IR_L L\left(\frac{1}{6} - \sum_{n=1}^{\infty}\frac{1}{(\pi n)^2}\exp\left(-\left(\frac{\pi n}{L}\right)^2\frac{q}{R_L C_L I}\right)\cos\left(\frac{\pi n}{L}x\right)\right). \qquad (21)$$

From equation (21), at x = 0, according to the model, Fig. 4, we obtain an expression for the voltage at accumulator terminals at its discharge by direct current in the form

$$U = E - \frac{q}{C_{CR}} - \frac{Ir}{3}\left(1 - \sum_{n=1}^{\infty}\frac{6}{(\pi n)^2}\exp\left(-\frac{(\pi n)^2 q}{rC_{CR}I}\right)\right). \qquad (22)$$

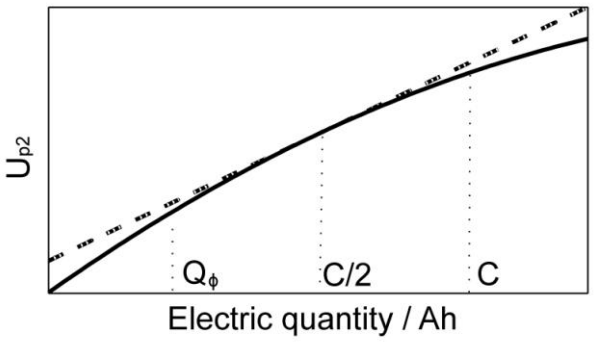

Figure 5. Dependency of discharge polarization summand from the quantity of transferred electricity for the KPL-55 type accumulators (dotted line marks possible linear substitution of the given dependency). Q_φ - quantity of transferred electricity from which the linear section of discharge curve starts; C – total discharge accumulator capacitance.

Because of the presence of infinite sum in the relations (22), it is not convenient to use it. This sum can be approximately calculated using Euler-Maclaurin summation formula [31]. Hence, we obtain

$$U = E - \frac{q}{C_{CR}} - \frac{Ir}{3}\left[1 - \exp(-a) + \frac{6}{\pi}\sqrt{\frac{a}{\pi}}(1 - erf(\sqrt{a}))\right], \qquad (23)$$

$$a = \frac{\pi^2 q}{rC_{CR}I}.$$

The first two summands (23) correspond to similar summands of Tremblay formula (2, 8). This model does not consider the ohmic resistance of electrolyte in the inter-electrode space. Let us treat the meaning of the third summand. Quality change of this summand depending upon q is represented in Fig. 5.

Thus, this summand at linear section of discharge curve can be quite precisely substituted with a straight line, expanding the additional summand into the Taylor's series in the point $q = C/2$. Hence, we obtain

$$U_{p2}=P(I)+H(I)q, \qquad (24)$$

where

$$H(I) \approx \frac{1}{C_{CR}}\left[\exp(-b)+\sqrt{\frac{\pi}{b}}\left(1-erf(\sqrt{b})\right)\right], \qquad (25)$$

$$P(I) \approx \frac{\pi^2 C}{6bC_{CR}}\left[1-\left(1+\frac{3b}{\pi^2}\right)\exp(-b)+\frac{3}{\pi}\sqrt{\frac{b}{\pi}}\left(1-erf(\sqrt{b})\right)\right], \qquad (26)$$

$$b = \frac{\pi^2 C}{2rIC_{CR}}.$$

Error function *erf(x)* at the interval $0 < x < \infty$ can be approximated by rational functions [32], whereas for the approximation error, the following estimate is true

$$|\varepsilon(x)| < 2.5\times 10^{-5}, \qquad (27)$$

which is quite sufficient for practical purposes.

Eventually, the relations (22) for the polarization discharge can be approximated as follows

$$U = E - P(I) - \frac{q}{C_{CR}}\left[1+\left(1+\sqrt{\frac{\pi}{b}}(a_1 t + a_2 t^2 + a_3 t^3)\right)\exp(-b)\right], \qquad (28)$$

where

$t = \frac{1}{1+p\sqrt{b}}$, p=0,47047, a_1=0,3480242,

a_2=-0,0958798, a_3=0,7478556.

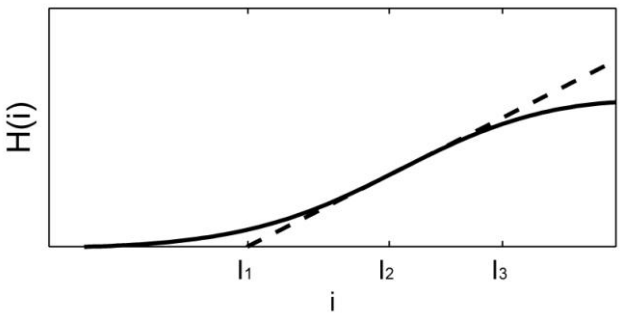

Figure 6. Dependency of additional slope coefficient for linear section of discharge curve from discharge current value for the accumulators type KPL55.

Summand *P(I)* provides an additional input into the activation-ohmic part, and does not influences the discharge curve slope. At high currents, *P(I)* function has the view of a linear dependency, i.e.

$$P(I) = A_0 + B_0 I, \quad (29)$$

where A_0, B_0 – certain constants.

The qualitative view of the function *H(I)* graph is shown in Fig. 6.

It can be observed from Fig. 6 that until the discharge current

$$I_1 = \frac{\pi^2 C}{8rC_{CR}}. \quad (30)$$

It is possible to ignore the slope coefficient input into the inclination of discharge curve linear section. Consequently, in the discharge currents' interval,

$$0 < I < I_1. \quad (31)$$

The discharge curves for any types of nickel-cadmium accumulators shall be well described by Tremblay equation.

Let's analyse relations (31). As for linear section of discharge curve

$$C_{CR} = \frac{C}{\psi_0}, \qquad r = \rho\frac{L}{S}, \quad (32)$$

where ψ_0 – linear part of voltage change at the accumulator discharge in the interval $0 < q < C$. Then, the relations (31) can be written in the following view

$$0 < I < \frac{\pi^2 \Psi_0 S}{8r\rho L}. \quad (33)$$

The value ψ_0 is determined by the electro-chemical nature of particular active substances of a certain type of accumulator. Consequently, for all the nickel-cadmium accumulators, ψ_0 is approximately equal [23]. From (33) it is observed that the less is the thickness of electrodes $2L$ and bigger their effective total surface area S (starter type accumulators), then in the broader interval of discharge currents, starting from zero, the Tremblay equation is true (2). As it was experimentally shown in Table 1, for KSX 25 accumulator, this is true up to the discharge currents $I = C_N$. From the other side, the bigger is the thickness of the electrodes $2L$, and smaller the total surface area S, then at the lower currents, the relations (33) shall become non applicable.

In the area

$$\frac{\pi^2\psi_0}{8r} = I_1 \le I \le I_3 = \frac{\pi^2\psi_0}{2r}, \quad (34)$$

function *H(I)* approximately has linear dependency of *I*, Fig. 6

$$H(I) = b_1 + a_1 I. \quad (35)$$

In the point

$$I_2 \approx 0.7\frac{\pi^2\psi_0}{2r}, \quad (36)$$

curve *H(I)* has an inflection, Fig. 6.

For this interval, the relations (28) shall take the view

$$U = E - \frac{q}{C_{CR}}(b_2 + a_2 I), \quad b_2 = 1 + C_{CR}b_1, \quad a_2 = C_{CR}a_1. \quad (37)$$

Consequently, the discharge polarization of GER equation (7) type appears, and the slope coefficient of linear section of the curve

$$k = (b_2 + a_2 I)/C_{CR} \text{ .} \quad (38)$$

shall grow linearly with the current discharge growth.

Relations (37) is equivalent to empirical equation (7) at

$$D = \frac{b_2 C}{C_{CR0}}, \qquad K = \frac{a_2 C}{C_{CR0}} \text{ .}$$

If it is possible to ignore the summand b_2 in comparison to $a_2 I$ (which is always possible at high currents) in relations (37), then the discharge polarization (37) unequivocally transfer into the Shepherd's discharge polarization (6), at $K = a_2 C/C_{CR0}$.

As observed in the experimental data (Table 4) for KPL-55 accumulator approximately within the interval of discharge currents from $0.1C_N$ to $0.5C_N$, the Shepherd's equation is true (optimal coefficient *K* of relations (6) does not change greatly at the change of discharge mode within the given interval). Consequently, the slope coefficient of linear section of discharge curve actually grows linearly with the increase in discharge current.

Hence, the interval defined in equation (34) corresponds to Shepherd's discharge model.

In the interval

$$I >> \frac{\pi^2 \psi_0}{2r} \text{ ,} \quad (39)$$

function *H(I)* grows as

$$H(i)=AI^m, \quad (40)$$

where $0.5 \le m < 1$, whereas at $I \to \infty$, $m \to 0.5$. This corresponds well to experimental data for KPL 55 accumulator at discharge currents $I >> 0.5C_N$ (Table 4).

Certainly, the summand in square brackets in the formula (28) accounts for decrease of depth of electro-chemical process penetration with the growth of external current. It is actually possible to introduce the effective capacitance in the form of

$$C_{CRef} = \frac{C_{CR}}{\left\{1 + \left[\sqrt{\frac{\pi}{b}}(a_1 t + a_2 t^2 + a_3 t^3) + 1\right]\exp(-b)\right\}} \text{ .} \quad (41)$$

From relations (41), it can be observed that with the growth of external discharge current, the accumulator capacitance drops and tends to zero, i.e. with the growth of discharge current, the smaller and smaller part of active substance takes part in electro-chemical process, which corresponds to the studies [28,29]. Whereas, at discharge current $I \to 0$, $C_{CRef} \to C_{CR}$.

Thus, this research shows that the empirical equations (1-3) do not contradict one another, but rather complement each other, as they are true for any alkaline battery, each in its range of discharge currents.

6. RELAXATION POLARIZATION

The last element of the accumulator block diagram, Fig. 1, describes development of transition processes in the accumulator at its switching for discharge. Analytical relations, describing this element operation, have similar view in Shepherd's (1), Tremblay (2), and GER (3), namely:

$$U_r = A\left(exp\left(-\frac{Bq}{C} \right) - 1 \right). \qquad (42)$$

In electro-technics, the relaxation processes are most frequently described by the diagrams of the type at Fig. 7(a), i.e. leaky condenser.

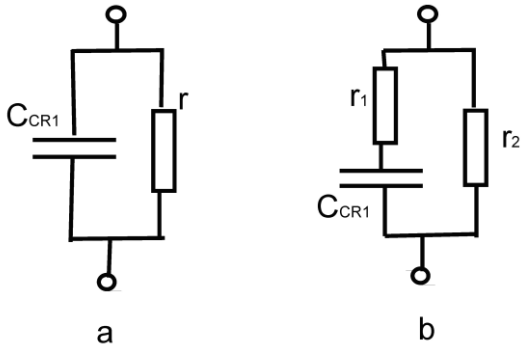

Figure 7. Possible structural diagrams of the relaxation element of the accumulator structural model. C_{CR1} – condenser; r, r_1, r_2, – resistances

Let us find voltage change at the given diagram by passing direct current through it. The main equation shall have the following view

$$-I = \frac{U}{r} + C_{CR1}\frac{dU}{dt}. \qquad (43)$$

Solution of this equation at the initial condition

$$U\big|_{t=0} = 0, \qquad (44)$$

shall be

$$U = -Ir\left(1 - exp\left(-\frac{q}{C_{CR1}Ir} \right) \right), \qquad (45)$$

where I – constant external current.

If we assume that the resistance r is created by a certain activation process that obey the Tafel equation

$$U = a + b\,ln(I), \qquad (46)$$

then, we may approximately consider r equal to the differential resistance for dependency (46), i.e.

$$r = \frac{dU}{dI} = \frac{b}{I}. \qquad (47)$$

Substituting (47) into (45), we obtain

$$U = b\left(\exp\left(-\frac{q}{C_{CR1}b} \right) - 1 \right). \qquad (48)$$

This dependency completely coincides with experimental dependency (42) at

$A=b$, $\quad B = \frac{C}{C_{CR1}b}$.

Consequently, the relaxation process in the accumulator can be described by the diagram Fig. 7(a), i.e. a certain leaking condenser. Whereas the leakage is connected with an activation process, adhering to Tafel equation.

From the electro-chemical point of view, the diagram of the relaxation element, Fig. 7(a), is incorrect. As explained in the third part, to describe an electro-chemical reaction in structural modelling, we need to use a pseudo-condenser. But any electro-chemical process is related to activation process, which is described by the so called Butler–Volmer equation, a particular case of which being the Tafel equation (46). Consequently, any structural model of an accumulator must contain a nonlinear resistance, modelling the activation process, successively connected with the pseudo-condenser, i.e. the structural diagram of the relaxation block of the accumulator, Fig. 1, should have the structure that is somewhat similar to Fig. 7(b).

The general equation for this diagram shall be

$$\frac{dU}{dt}+\frac{1}{(r_1+r_2)C_{CR1}}U=-\frac{Ir_2}{C_{CR1}(r_1+r_2)}. \qquad (49)$$

Solution of the given equation at the initial condition (in the moment of switching for discharge the resistance of the condenser is zero)

$$U\big|_{t=0}=-I\frac{r_1r_2}{r_1+r_2} \qquad (50)$$

shall have the view

$$U=\frac{Ir_2^2}{r_1+r_2}\left(\exp\left(-\frac{q}{(r_1+r_2)C_{CR1}I}\right)-1\right)-I\frac{r_1r_2}{r_1+r_2}. \qquad (51)$$

Once again, if resistances r_1 and r_2 are created by the activation process, obeying Tafel equation (i.e. they have the view (47)), the first summand of formula (51) coincides with the experimental dependency (42) at

$$A=\frac{b_2^2}{b_1+b_2},\qquad B=\frac{C}{C_{CR1}(b_1+b_2)}. \qquad (52)$$

Second summand (51) provides the input into the activation-ohmic element of the accumulator Fig. 1.

If

$$r_2>>r_1, \qquad (53)$$

from (51), we obtain

$$U=Ir_2\left(\exp\left(-\frac{q}{r_2C_{CR1}I}\right)-1\right)-Ir_1, \qquad (54)$$

i.e. relations (51) transfers into relations (45) (ignoring the activation-ohmic summand). As mentioned below, in real nickel-cadmium accumulator, the relations (53) are always true. Consequently, diagram Fig. 7(a) may be considered as an approximated diagram for a possible relaxation block Fig. 7(b).

On the basis of above analysis, block diagram at Fig. 1 and research from the previous sections, we may assume that complete structural model of an accumulator has the view Fig. 8(a), or the approximated view, Fig. 8(b).

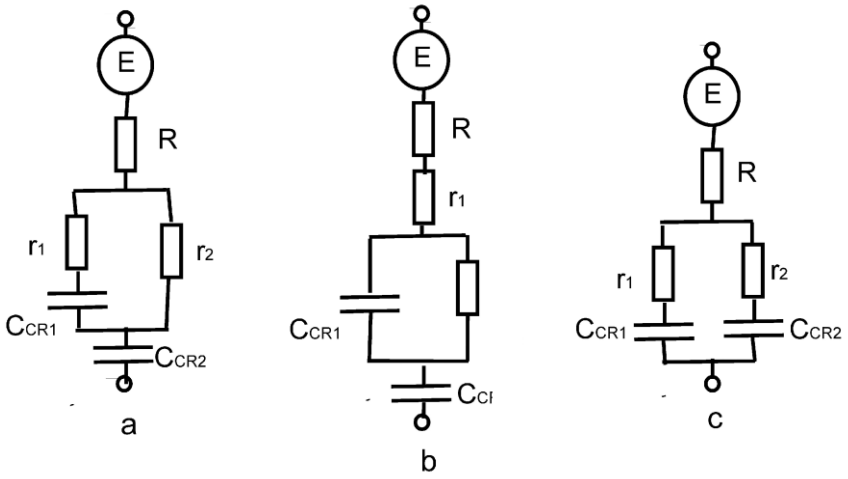

Figure 8. Possible complete structural accumulator models: R – electrolyte resistance in the inter-electrode space; C_{CR2} – main pseudo-condenser, corresponding to the main current-forming electro-chemical reaction (13) (distribution of the main pseudo-condenser along the depth of porous electrode is not considered); r_1, r_2, C_{CR1} – elements of relaxation block and E – accumulator EMF

However, from electro-chemical point of view, complete structural models of an accumulator Fig. 8(a, b) are not true. In fact, the pseudo-condenser C_{CR1} models a certain electro-chemical reaction, and as the result of any electro-chemical reaction, one or several electrons shall pass to the metallic matrix of the electrode. But according to the Fig. 8(a, b), these electrons shall move in the direction of the pseudo-condenser C_{CR2} and consequently, participate in the second electro-chemical reaction, which is impossible. It turns out that the first electro-chemical reaction takes place not on the electrode, and it does not possess electro-chemical sense. Hence, if several pseudo-condensers are present (describing several electro-chemical reactions) in the general structural model of an accumulator, they must have a parallel connection. In addition, one of the plates of pseudo-condensers shall be connected to a free terminal, which shall correspond to the possibility of transition of electrons obtained in the result of electro-chemical reaction onto the metallic matrix of electrodes. The simplest complete structural model of an accumulator corresponding to these conditions appears as shown in Fig. 8(c).

The system of equations, describing processes in the ring portion of diagram, Fig. 8(c), can be written in the following view

$$\begin{cases} -I = I_1 + I_2 \\ I_1 = C_{CR1}\dfrac{dU}{dt} - C_{CR1}r_1\dfrac{dI_1}{dt} \\ \dfrac{dI_1}{dt} + \dfrac{(C_{CR1}+C_{CR2})}{(r_1+r_2)}\dfrac{I_1}{C_{CR1}C_{CR2}} = -\dfrac{I}{C_{CR2}(r_1+r_2)} \end{cases}, \qquad (55)$$

where I – constant external current and I_1 and I_2 – currents in parallel branches. The initial conditions for this system of equations shall be

$$U\big|_{t=0} = -\frac{r_1 r_2}{(r_1 + r_2)} I,$$
$$I_1\big|_{t=0} = -\frac{r_2}{(r_1 + r_2)} I. \qquad (56)$$

Solutions of the system of equations (55) shall have the following view

$$U = -\frac{q}{C_{CR1} + C_{CR2}} + I\left[\frac{C_{CR2}(r_1 + r_2)}{C_{CR1} + C_{CR2}} - r_1\right]\cdot\left[\frac{r_2}{r_1 + r_2} - \frac{C_{CR1}}{C_{CR1} + C_{CR2}}\right]\times$$
$$\times\left(\exp\left(-\frac{(C_{CR1} + C_{CR2})}{C_{CR1} C_{CR2}(r_1 + r_2)}\frac{q}{I}\right) - 1\right) - I\frac{r_1 r_2}{(r_1 + r_2)}. \qquad (57)$$

The first summand of the relations (57) describes the discharge polarization. This summand was examined in detail in Sections 3–5. The last summand provides input into the activation-ohmic element of the accumulator. The second summand shall describe the relaxation polarization (42) if resistances r_1 and r_2 have the view (47), i.e. describe the activation processes, obeying to Tafel equation (46).

At

$$C_{CR2} >> C_{CR1}, \qquad (58)$$

the second and the third summands of the relations (57) transfer into relations (51). As it is shown below, in the real accumulator, the relation (58) is fulfilled quite well. Consequently, the structural models, Fig. 8(a, b), can be evaluated as approximated models of the accumulator, true under condition (58) or (53), accordingly.

The structural model of an accumulator Fig. 8 (c) has a highly visual electro-chemical interpretation. It describes two parallel electro-chemical reactions: r_2 and C_{CR2} – activation resistance and pseudo-capacitance of the main current-forming reaction (13), and r_1 and C_{CR1} – activation resistance and pseudo-capacitance of the parallel (unknown) electro-chemical reaction.

It is possible to make the following conclusions out of the above research.

1. Availability of the relaxation summand (42) in empirical equations (1–3), from the point of view of structural modelling, unequivocally confirms the existence of an electro-chemical reaction, parallel to the main current-forming reaction (13) at accumulator charging and discharge.

2. Parallel electro-chemical reaction is the cause of appearance of initial nonlinear section of discharge curve, which is described by the relaxation summand (42).

We shall yet omit the electro-chemical nature of the parallel reaction, but should investigate the conditions to which this reaction shall correspond, using experimental discharge curves of the accumulators as the criterion. According to the research in Sections 4–5, the pseudo-condenser C_{CR2} determines the slope angle of discharge curve linear section. The pseudo-condenser C_{CR1} shall determine the slope angle of discharge curve linear section in the moment of switching the accumulator for discharge as it is particularly responsible for the relaxation process, which is on at this moment.

It follows that in the moment of switching the accumulator for discharge, the current shall mostly pass through pseudo-condenser C_{CR1}, and it happens only under the condition when

$$r_1 << r_2. \qquad (59)$$

In this case, out of (57), we receive

$$\left.\frac{dU}{dq}\right|_{t=0} \approx -\frac{1}{C_{CR1}} . \qquad (60)$$

As the slope angle of discharge curve in the moment of switching the accumulator for discharge exceeds (by absolute value) the slope angle of linear section of discharge curve

$$\left.\frac{dU}{dq}\right|_{q=\frac{C}{2}} \approx -\frac{1}{C_{CR2}},$$

then, it follows that in the real accumulator

$$C_{CR2} >> C_{CR1}. \qquad (61)$$

Thus, for the real accumulator, the conditions (59) and (61) should be satisfied. Only in this case, the observed experimental discharge curves can be obtained.

From the obtained equations (59) and (61), we can draw three conclusions.

First, from equation (59), it is followed that the potential barrier separating hydroxyl ions in the composition of substance obtained as the result of parallel electro-chemical reaction from hydroxyl ions in free solution is considerably lower than the potential barrier separating hydroxyl ions in the composition of nickel and cadmium hydroxides from hydroxyl ions in free solution, i.e. in the result of the parallel electro-chemical reaction, we obtain a substance, which is very less stronger than nickel and cadmium hydroxides.

Second, from equation (59), it follows that at charging of the nickel-cadmium accumulator, voltage at pseudo-condenser C_{CR1} shall be always higher than at pseudo-condenser C_{CR2}. Consequently, for example, at charging of oxide-nickel electrode as the result of the parallel electro-chemical reaction, a more oxygenised phase than the main nickel hydroxides (according to reaction (13)) is obtained. In contrast, on the cadmium electrode at charging, the less oxygenised phase than the main cadmium hydroxides shall form.

Third, according to (61), capacitance of the parallel electro-chemical reaction shall be much smaller than capacitance of the main electro-chemical reaction (13). Hence, it shall not influence the capacitance of the complete accumulator. However, the formed unstable phase shall provide the considerable influence to the alternating-current and relaxation processes in the accumulators.

It is a well-known fact that as the result of the charging of the nickel-cadmium accumulators, e.g. on the oxide-nickel electrode, the highly oxygenised unstable phase forms. It is due to its disintegration and redistribution of charge along the depth of porous electrode, the difference of potentials at the accumulator terminals decreases after its charging [22–25, 28, 33].

However, the detailed study and clarification of the nature of parallel electro-chemical reaction requires vast additional research.

Structural models of an accumulator, Fig. 8(a, b), can also have practical application as they are the approximations of the model Fig. 8 (c), which is true under the conditions (61) and (59). As it is mentioned above, these conditions are always true for real nickel-cadmium accumulators.

7. DISCUSSION

Relaxation polarization (42) does not depend on discharge current; that is, at any discharge current, it has one and the same view. As explained in Section 5, the dependency from discharge current develops only when an electrochemical reaction is distributed along the depth of a porous electrode. Consequently, the electrochemical reaction responsible for relaxation polarization is not distributed along the depth of a porous electrode but is concentrated in the surface layers of the electrode. This conclusion corresponds to the research [23,28,29]. Hence, for example, during the charging of the nickel-cadmium accumulator, the unstable highly oxygenized phase forms only at the surface of the oxide-nickel electrode. Disintegration of this phase and redistribution of the degree of oxidation of nickel hydroxide will cause a decrease of potential difference at the accumulator terminals just after accumulator charging, which is exactly what is observed in experiments. Consequently, in the complete structural model of an accumulator, it is necessary to consider the distribution only of the main electrochemical reaction (13) along the depth of the porous electrode and not to consider the distribution of the parallel reaction responsible for relaxation processes. Thus, on the basis of all the performed research, the complete structural model of an accumulator appears as shown in Fig. 9.

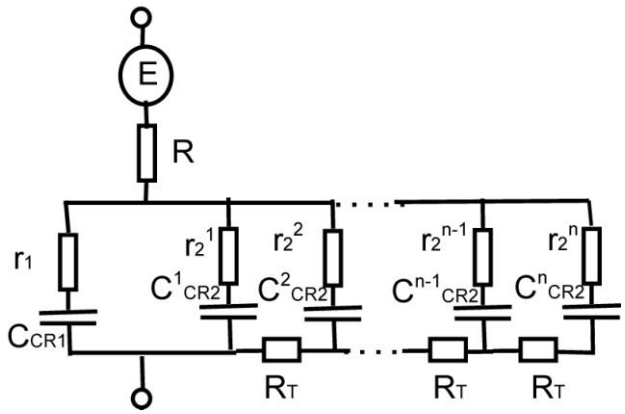

Figure 9. Accumulator nonlinear structural model. E – accumulator EMF, R – electrolyte resistance in the inter-electrode space; C_{CR2}^{i}, r_2^i – distribution of main pseudo-condenser and activation resistance along the depth of porous electrode (corresponding to the main current-forming electro-chemical reaction (13)); C_{CR1}, r_1 – pseudo-condenser and activation resistance of electro-chemical reaction responsible for relaxation processes in the accumulator and R_T – resistance to transport of ions into the depth of electrode along the liquid phase and active substance.

It is necessary to note especially that the received structural model of the accumulator (Fig.9) fundamentally differs from equivalent circuits of accumulators used in statistical and constructive models [34-37]. In the equivalent circuit, many elements do not correspond to any objects or processes in the accumulator. The task of the equivalent circuit is to display the found empirical dependence. Therefore, the given circuits may be used, as statistical models that are equivalent to them, only within the framework of the solved problem. They cannot be used for the calculation of other modes of the operation of an accumulator in an area where the used empirical correlations are not correct.

Equivalent circuits of accumulators were widely used for 60–80 years. However, they are now often used for the modeling work of accumulators in the structure of electric and hybrid vehicles within the limits of statistical and constructive models [13,14, 34,35].

In the structural model, each element describes an object, a process, or a stage of process in the accumulator. Therefore, the structural models use the elements whose behavior is equivalent to the behavior of the real objects of the system under study, irrelevant of the mode of operation of the system. Consequently, these models possess the same wide area of applicability as the dynamic models.

In our article [38], the structural model accumulator in Fig. 9 has been successfully used for modeling the self-discharge accumulators. It was demonstrated that existing empirical equations for the self-discharge process are special cases of a general solution of the structural model in Fig. 9. Furthermore, it was demonstrated that the empirical equations do not contradict each other; rather, they supplement each other, as each is correct over a different time interval of self-discharge. This model is convenient for modeling the operation of electric and hybrid vehicles [13,14]. This work appears to be a continuation of works [39,40] devoted to analytical modeling of accumulators' various operational modes.

8. CONCLUSIONS

The structural model in Fig. 9 is developed based on the empirical equations (1–3) and the well-known fact that the electrochemical process is distributed along the depth of a porous electrode [4-10]. However, the equations (1–3) are applicable for acid, Li-Ion, and NiMH accumulators [13,14,21] and the electrodes of almost all the accumulators are porous. Due to this, it is possible to assume that the structural model in Fig. 9 is applicable for the accumulators of other electrochemical systems. Nevertheless, this assumption needs separate theoretical and experimental research, as in this article and article [34] it was verified only for nickel-cadmium accumulators.

References

1. N. Achaibou, M. Haddadi and A. Malek, *J. Power Sources*, 185 (2008) 1484
2. I. De Michelis, F. Ferella, E. Karakaya, F. Beolchini and F. Vegli`o, *J. Power Sources*, 172 (2007) 975
3. J. Schiffer, D.U. Sauer, H. Bindner, T. Cronin, P. Lundsager and R. Kaiser, *J. Power Sources*, 168 (2007) 66
4. M. Cugnet, S. Laruelle, S. Grugeon, B. Sahut, J. Sabatier, J-M. Tarascon and A. Oustaloup, *J. Electrochem. Soc.,* 156 (2009) A974
5. K. Siniard, M. Xiao and S-Y. Choe, *J. Power Sources*, 195 (2010) 7102
6. M. Venkatraman and J.W. Van Zee, *J. Power Sources*, 166 (2007) 537
7. T.G. Zavalis, M. Behm and G. Lindbergh, *J. Electrochem. Soc.*, 159 (2012) A848-A859
8. V. Boovaragavan, R.N. Methakar, V. Ramadesiga and V.R. Subramanian, *J. Electrochem. Soc.*, 156 (2009) A854-A862
9. P. Albertus, J. Couts, V. Srinivasan and J. Newman, *J. Power Sources*, 183 (2008) 771

10. J. F. Johansen, T. W. Farrell and C.P. Please, *J. Power Sources*, 156 (2006) 645
11. J. Kowal, D. Schulte, D.U. Sauer and E. Karden, *J. Power Sources*, 191 (2009) 42
12. A. Hausmann and C. Depcik, *J. Power Sources*, 235 (2013) 148
13. O. Tremblay, L.-A. Dessaint and A.-I. Dekkiche, *Vehicle Power and Propulsion Conference, VPPC 2007. IEEE*, Arlington, USA, 9-12 Sept. (2007) 284
14. O. Tremblay and L.-A. Dessaint, *World Electric Vehicle Journal*, 3 (2009) 2
15. M. Thele, J. Schiffer, E. Karden, E. Surewaard and D.U. Sauer, *J. Power Sources*, 168 (2007) 31
16. A. Vasebi, M. Partovibakhsh and S.M. Taghi Bathaee, *J. Power Sources*, 174 (2007) 30
17. M.A. Roscher and D.U. Sauer, *J. Power Sources*, 196 (2011) 331
18. D. Andrea, M. Meilera, K. Steinera, H. Walza, T. Soczka-Gutha and D.U. Sauerb, *J. Power Sources*, 196 (2011) 5349
19. S.M. Rezaei Niya, M. Hejabi and F. Gobal, *J. Power Sources*, 195 (2010) 5789
20. J.R. Scully, D.C. Silverman and M.W. Kendig (Eds), *Electrochemical Impedance: Analysis and Interpretation*, ASTM, Philadelphia (1993)
21. C.M. Shepherd, *J. Electrochem. Soc.*, 112 (1965) 657
22. R. Kaiser, *J. Power Sources*, 168 (2007) 58
23. L.E. Unnewehr and S.A. Nasar, *Electric Vehicle Technology*, John Wiley & Sons, New York (1982)
24. *Termo_Analytics_Inc. Battery Modeling*, http://www.thermoanalytics.com/docs/batteries.html
25. J.B. Copetti, E. Lorenzo and F. Chenlo, *Progress in Photovoltaics*, 1 (1993) 283
26. *SimPowerSystems Reference Hydro-Québec*, http://www.mathworks.com/access/helpdesk/help/pdf_doc/physmod/powersys/powersys_ref.pdf p.2-40
27. E.A. Hyman, *U.S. Department of Energy*, DC, Washington (1977)
28. N.E. Galushkin and Y.D. Kudriavtsev, *Russian Journal of Electrochemistry*, 30 (1994) 344
29. N.E. Galushkin and Y.D. Kudriavtsev, *Russian Journal of Electrochemistry*, 33 (1997) 559
30. T.W. Farrell, L.S. Mcelwain, A.J. Swinkels and A. Finite, *Journal of Applied Mathematics and Decision Sciences*, 5 (2001) 119
31. G.A. Korn and T.M. Korn, *Mathematical Handbook for Scientists and Engineers*, McGraw-Hill Book Co, New York (1968) 126
32. M. Abramowitz and I.A. Stegun (Eds), *Handbook of Mathematical Functions With Formulas, Graphs, and Mathematical Tables, NBS Applied Mathematics Series*, National Bureau of Standards, Washington (1964) 298
33. N.E. Galushkin and Y. D. Kudriavtsev, *Russian Journal of Electrochemistry*, 29 (1993) 1115
34. R. Garcia-Valle and J.A. Pecas Lopes (Eds), *Electric Vehicle Integration into Modern Power Networks, Power Electronics and Power Systems*, Springer Science+Business Media, New York (2013)
35. Y. Xing, E.W. Ma, K.L. Tsui and M. Pecht, *Energies*, 4 (2011) 1840
36. J. Zhang and J. Lee, *J. Power Sources*, 196 (2011) 6007
37. M. Amiria, M. Esfahanianb, M.R. Hairi-Yazdic and V. Esfahanianc, *J. Power Sources*, 190 (2009) 372
38. N.E. Galushkin, N.N. Yazvinskaya and D.N. Galushkin, *J. Electrochem. Soc.*, 159 (2012) A1315
39. N.E. Galushkin, N.N. Yazvinskaya and D.N. Galushkin, *Int. J. Electrochem. Sci.*, 9 (2014) 1911
40. N.E. Galushkin, N.N. Yazvinskaya, D.N. Galushkin and I.A Galushkina, *Int. J. Electrochem. Sci.*, 9 (2014) 4429